ELSEVIER

Colloids and Surfaces B: Biointerfaces 13 (1999) 37–45

COLLOIDS AND SURFACES B

Interfacial and/or molecular recognition by lipases of mixed monomolecular films of 1,2-dicaprin and chiral organophosphorus glyceride analogues?

Frank Marguet [a], Isabelle Douchet [b], Jean-François Cavalier [a], Gerard Buono [a], Robert Verger [b,*]

[a] *ENSSPICAM, UMR 6516, 'Synthèse, Catalyse et Chiralité' avenue Escadrille Normandie-Niemen, F-13397 Marseille Cedex 20, France*

[b] *Laboratoire de Lipolyse Enzymatique, UPR 9025, IFR 1 du CNRS, 31, Chemin Joseph Aiguier, F-13402 Marseille Cedex 20, France*

Accepted 2 December 1998

Abstract

Enantiomerically pure *sn*-1,2- and *sn*-2,3-*O*-didecanoylphosphonoglycerides, were synthesised and investigated as inhibitors of human pancreatic lipase (HPL) and human gastric lipase (HGL). The inhibition studies were performed using the monomolecular film technique coupled with ELISA tests. All the four stereoisomers investigated reduced the hydrolysis of 1,2-dicaprin by both lipases. With HPL, they exhibited a rather weak inhibitory power and no significant differences were observed among them. With HGL, the inhibition depended much more strongly on the chirality at the *sn*-2 carbon of the glycerol backbone, while the chirality at the phosphorus had no influence. Moreover, a clear correlation was observed between the HGL surface concentration and the inhibitor surface molar fraction (α_{50}) leading to half inhibition. The greatest enzymatic inhibition was observed with films containing the enantiomeric inhibitor to which the HGL was best adsorbed, assuming thus that the interfacial lipase binding was controlled by a supramolecular chiral recognition process.

Keywords: Acylglycerol analogues; Phosphonates; Human pancreatic lipase; Human gastric lipase; Inhibition kinetics; Monomolecular lipid films

1. Introduction

Many of the natural phospholipids, which are the building blocks of biological cell membranes, are chiral, and their chirality is known to be of importance to the interactions of the cell membrane with proteins and other substances passing through it [1–3]. In order to better understand such phenomenon of chiral recognition at interfaces, we used a model system consisting of water soluble enzymes (lipases) and water insoluble chiral inhibitors spread as monomolecular films.

* Corresponding author. Fax: +33-491-715-857; e-mail: verger@ibsm.cnrs-mrs.fr.

0927-7765/99/$ - see front matter
PII: S0927-7765(98)00099-X

Patkar and Bjorkling [4] reviewed several families of lipase inhibitors including boronic acids, phosphorus-containing inhibitors and β-lactone-containing inhibitors. The inhibition could be monitored by *p*-nitrophenol release from ethyl *p*-nitrophenyl hexylphosphonate. Quantitative analysis of the data indicated that a 1:1 lipase–inhibitor complex was formed during inhibition. Enantioselective inhibition was found for the lipases from *Candida antarctica* and *Rhizomucor miehei* using pure enantiomers of ethyl *p*-nitrophenyl hexylphosphonate as inhibitors. These phosphonates can be regarded as true active site-directed inhibitors. The inhibited enzymes can be said to be analogues of the tetrahedral intermediate in the acylation step that occurs during triacylglycerol hydrolysis.

1,2-Dioctylcarbamoylglycero-3-*O*-*p*-nitrophenyl alkylphosphonates, where the alkyl is a methyl or octyl group, were synthesised and their activity was tested as irreversible inhibitors of cutinase from *Fusarium solani pisi* and *Staphylococcus hyicus* lipase by Mannesse et al. [5]. Rapid inhibition of these enzymes occurred with a concomitant release of one mol of *p*-nitrophenol per mol of enzyme. Both lipases show great selectivity towards the chirality of these compounds at the glycerol and phosphorus sites.

Stadler et al. [6] synthesised 1,2(2,3)-diradylglycero-*O*-(*p*-nitrophenyl) *n*-hexylphosphonates, with the diradylglycerol moiety being di-*O*-octylglycerol, 1-*O*-hexadecyl-2-*O*-pyrene-decanoylglycerol, or l-*O*-octyl-2-oleoylglycerol, and tested for their ability to inactivate lipases from *Chromobacterium viscosum* and *Rhizopus oryzae*. The experimental data indicate the formation of stable, covalent 1:1 enzyme-inhibitor adducts with the di-*O*-alkylglycero phosphonates. Both lipases exhibited the same preference for the chirality at the phoshorus that was independent from the absolute configuration at the glycerol backbone.

A fungal lipase from *Candida rugosa* has been crystallized with and without inhibitor, revealing a similar structural modification: the helical lid has to be shifted in order to unmask a buried active site [7–9]. Furthermore, using both enantiomers of menthyl hexylphosphonate as inhibitors of *C. rugosa* lipase, Cygler et al. [9] established a structural basis for the chiral preferences of lipases.

Recently, Longhi et al. have crystallized a cutinase from *F. solani* with a triacylglycerol analogue: (*R*)-1,2-dibutyl-carbamoyl glycero-3-*O*-*p*-nitrophenyl butyl phosphonate. This inhibitor is covalently linked to the active site serine, mimicking the first tetrahedral intermediate along the reaction pathway. This structure provides a more realistic model for a complex between a lipolytic enzyme and a triacylglycerol [10].

Various lipase inhibitors were synthesised by Marguet et al. [11,12], replacing the carbonyl of the hydrolysable ester bonds by a phosphonate group with a good leaving group and were investigated as potential inhibitors of human pancreatic lipase (HPL) and human gastric lipase (HGL). In an attempt to further characterize the active site and catalytic mechanism of pancreatic lipase, a C_{11} alkyl phosphonate compound was selected as an effective inactivator. The crystal structure of the pancreatic lipase–colipase complex inhibited by this compound was determined at a resolution of 2.46 Å [13]. As was observed in the case of the structure of the ternary pancreatic lipase–colipase–phospholipid complex [14], the binding of the ligand induces rearrangements of two surface loops in comparison with the closed structure of the enzyme [15]. The inhibitor, which could be clearly observed in the active site, was covalently bound to the active serine 152.

In view of the above results, 1,2-diacyl-3-phosphonoglycerides, which are true acylglycerol analogues (Fig. 1), were synthesised and tested as potential inhibitors of HPL and HGL.

2. Materials and methods

2.1. Materials

1,2-Didecanoyl-*sn*-glycerol (1,2-dicaprin) was purchased from Serdary Research Laboratory (Ont., Canada); Streptavidine peroxydase and *O*-phenilenediamine dihydrochloride were purchased from Sigma.

2.2. Lipases

HGL and HPL were purified at the laboratory using previously described procedures [16,17]. Monoclonal and polyclonal antibodies against either native HGL or native HPL were prepared and characterised as previously described [18–20].

2.3. Monomolecular film experiments

Before each utilisation, the Teflon trough was cleaned with tap water, then gently brushed in the presence of distilled ethanol, before being washed again with tap water and finally rinsed with double-distilled water. The aqueous subphase was composed of 10 mM Tris/HCl, pH 8, 100 mM NaCl, 21 mM $CaCl_2$ and 1 mM EDTA for HPL assays or 10 mM sodium acetate/HCl, pH 5, 100 mM NaCl, 21 mM $CaCl_2$ and 1 mM EDTA for HGL assays. Buffers were prepared with double-distilled water and filtered through a 0.45 μM Millipore membrane. Residual surface-active impurities were removed before each assay by sweeping and suction of the surface [21].

2.4. Enzymes kinetics experiments

Measurements were performed with the KSV 2200 Barostat equipment (KSV-Helsinki). The principle of the method has been described previously by Verger et al. [21]. It involved the use of a 'zero-order through' with two compartments: a reaction compartment and a reservoir compartment, which were connected to each other by a small surface channel. Enzyme solution was injected into the subphase of the reaction compartment only, whereas the lipid film covered both of them. A mobile barrier, automatically driven by the barostat, moved back and forth over the reservoir to keep the surface pressure (π) constant, thus compensating for the substrate molecules removed from the film by the enzyme hydrolysis. The surface pressure was measured on the reservoir compartment with a Wilhelmy plate (perimeter 3.94 cm) attached to an electromicrobalance, connected in turn to a microprocessor programmed to regulate the mobile-barrier movement. The reaction compartment was stirred at 250 rpm by two 2.5 cm magnetic bars. The surface of the reaction compartment was 100 cm^2 and its volume 100 ml. The reservoir compartment was 148 mm wide and 249 long. Mixed films of substrate/inhibitor were spread from a chloroform solution (~ 1 mg ml^{-1}), over the surface of the reaction compartment only, whereas the reservoir was covered with a film of pure substrate (1,2-dicaprin) [22–24]. The kinetics of hydrolysis were recorded for 20–25 min, and the kinetics data was analysed as in the case of a previous model [25–27]. Each experiment was performed in duplicate.

2.5. ELISA (enzyme linked immunosorbant assay) tests

The kinetics of hydrolysis were recorded as described above for 15 min, and the remaining film was aspirated as previously described [28]. The film was recovered (0.3–1 ml) into a glass tube by placing a barrier across the surface chan-

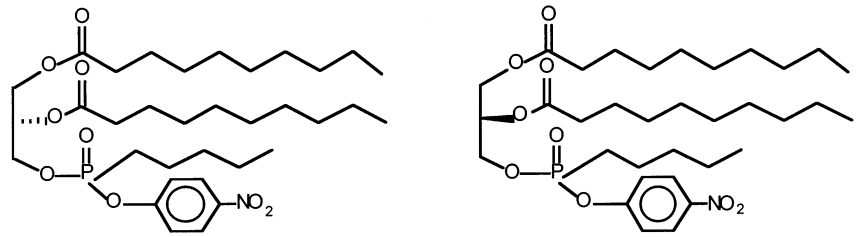

Fig. 1. Chiral phosphonates A, A′, B, B′ synthesised, analogous to triglycerides [12].

nel and by sweeping it over the reaction compartment and aspiring the film thus collected. After completely recovering the film, an equal volume of the sub-phase was sampled and placed in another tube. The difference between the total amount of proteins between these two samples was attributed to the surface excess of protein molecules bound to the lipid film.

All the ELISA tests were performed in 96-wells poly(vinylchloride) (PVC) microplates (Maxisorb, Nunc). The wells were coated with 250 ng of a specific polyclonal antibody (anti-HGL or anti-HPL for the titration of HGL and HPL, respectively) solubilized in 50 μl of 10 mM phosphate buffer (pH 7.5) containing 137 mM NaCl, 2.7 mM KCl and 8 mM Na_2HPO_4, 12 H_2O (buffer A) and incubated overnight at 4°C. The wells were then washed three times, each for 5 min, with 300 pl $well^{-1}$ of buffer A, and the excess protein binding sites were saturated by incubation with 200 μl $well^{-1}$ of blocking agent (3% w/v Regilait skimmed milk powders in buffer A) for 2 h at 37°C. The plates were then washed three times with buffer B (buffer A containing 0.05% v/v Tween 20), and dry the excess buffer by aspiration. Fill each well with 50 μl of sample solution in diluted buffer A, and incubate 1 h at 37°C. Wash the plates three times for 5 min with buffer B, and fill each well with 50 pl of specific monoclonal anti-HGL or anti-HPL (detector antibody) in buffer B, and keep at 37°C for l h. Wash three times for 5 min with buffer B, and fill each well with 50 μl of Streptavidine peroxydase diluted with buffer B at 1/1000. Keep at 37°C for 45 min. After washing the plates three times for 5 min with buffer B, and drying the excess buffer by aspiration, 50 μl of peroxydase substrate solution (*O*-phenylenediamine dihydrochloride 0.4 g l^{-1} in 100 mM sodium phosphate/150 mM sodium citrate (pH 5) containing 0.04% of fresh hydrogen peroxide) was added to each well and incubated for 15 min in the dark at room temperature. The enzyme reaction was stopped by adding 50 pl of 0.5 M H_2SO_4 to each well. The optical density (OD) was measured at 490 nm using a micro ELISA reader (MR 5000, Dynatech).

2.6. Determination of the amount of protein adsorbed to the lipid monolayer

A reference curve was drawn up for each test and was used to determine the amount of protein adsorbed to the lipid monolayer. For this purpose, biotinylated proteins (HGL* or HPL*) at known concentrations in 50 μl of buffer B were incubated in the wells of a micro-titration plate previously coated with a specific polyclonal antibody. An ELISA was performed as described above. The optical density values at 490 nm were plotted as a function of the concentration of protein. Each assay was carried out in duplicate. The obtained reference curve was used to calculate the concentration of protein in the aspirated samples recovered from the monomolecular experiments as described above. In order to calculate the amount of protein bound to the monomolecular lipid film, the volume occupied by the lipid film was not taken into account since it was negligible with respect to the aspirated sub-phase. We used the following equation:

$$\Gamma = \frac{[F+B]-[B]}{S} \cdot V_a$$

where Γ is the surface excess of protein bound to the lipid monolayer, expressed in ng cm^{-2}. $[F+B]$ is the concentration of protein present in the aspirated film with the aspirated bulk sub-phase, as determined by ELISA test. $[B]$ is the concentration of protein in the bulk sample, also determined by ELISA. V_a is the aspirated volume (ranging from 0.6 to 1.6 ml), and S the area of the reactional compartment of the through (100 cm^2).

2.6.1. Reliability of the sandwich ELISA for HGL* and HPL* adsorbed lipid monolayers

During the monolayers experiments, the validity of the sandwich ELISA for HGL* and HPL* was tested in the presence of mixed films of inhibitor/1,2-dicaprin. The recovery levels of protein injected under lipid monomolecular films were determined after each experiment as:

$$\text{Total recovery } (\%) = \frac{[B] \cdot V_t + \Gamma \cdot S}{T} \cdot 100$$

where $[B]$ is the concentration of HGL or HPL in the sub-phase; V_t is the total volume of the reactional compartment measured after each mono-

layer experiment (119 ± 9 ml); ΓS is the total amount of protein adsorbed to the monomolecular film; and T is the total amount of HGL* (9.9 μg) or HPL* (0.68 μg) injected under the monomolecular film.

3. Results and discussion

Enantiomerically pure *sn*-1,2- and *sn*-2,3-*O*-didecanoylglycerol were prepared and reacted with *n*-pentylphosphonic acid dichloride and *p*-nitrophenol to afford the corresponding diastereomeric phosphonates (Fig. 1). The separation of each phosphonates diastereomers A/B or A′/B′ were performed on a Waters HPLC system, using a silica gel column 250 × 10 mm 5 μm, and a Waters UV detector at 234 nm. The HPLC analysis were carried out at 25°C using *n*-heptane/2-propanol (99.05:0.95) as eluent; flow rate 3 ml min^{-1}. t_1(A or A′) = 24.5 min, [^{31}P]NMR: 30.4 ppm; t_2(B or B′) = 27.3 min, [^{31}P]NMR: 30.2 ppm.

Four enantiopure stereoisomers A, A′, B, B′ were then obtained, although the absolute configuration at the phosphorus has not yet been determined. It turned out that the behavior of neither of the lipases tested was influenced by the chirality at the phosphorus atom. We intentionally conserved the two carboxyl ester linkages in order to mimick as closely as possible the structure of acylglycerols (natural substrates). This decision turned out a posteriori to be justified, since negligible hydrolysis of these compounds occurred during the experiments carried out with HPL (5.0%) or HGL (2.3%).

The inhibition of HGL and HPL was studied using the monomolecular film technique [21–24] with mixed films of 1,2-dicaprin containing variable proportions of each of the four chiral organophosphorus compounds mentioned above. At the end of each kinetic experiment, the interfacial lipase binding was evaluated by ELISA tests using biotinylated lipases. The latter method was developed at our laboratory in order to measure the lipases surface density in the ng range [28]. In the presence of any of the four stereoisomers investigated, a decrease in the 1,2-dicaprin hydrolysis rate was systematically observed (Fig. 2).

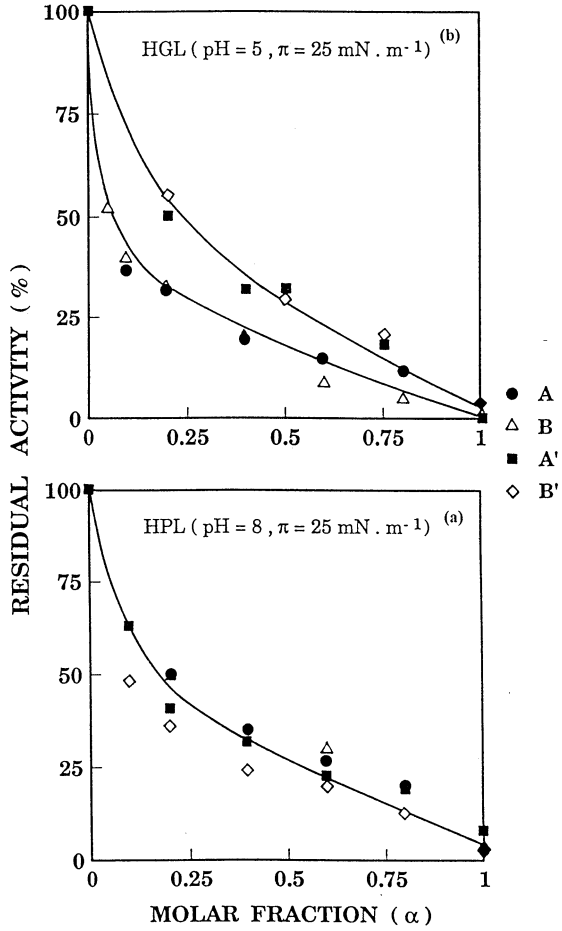

Fig. 2. Effect of increasing surface concentration of A(●), B(△), A′(■), B′(◇) on the hydrolysis rate of 1, 2-dicaprin monolayer at a constant surface pressure (25 mN m^{-1}) by HPL (a) and HGL (b). The aqueous subphase was composed of 10 mM sodium acetate/HCl, pH 5.0, 100 mM NaCl, 21 mM $CaCl_2$ and 1 mM EDTA in HGL assays, and 10 mM Tris/HCl, pH 8.0, 100 mM NaCl, 21 mM $CaCl_2$ and 1 mM EDTA in HPL assays. The kinetics of hydrolysis were recorded for 40–45 min. Each experiment was performed in duplicate as described in Section 2.

Furthermore, lower amounts of HPL and HGL were adsorbed on films of pure enantiomeric inhibitors than on pure 1,2-dicaprin films (Table 1).

With HPL (Fig. 2(a)), the four stereoisomers exhibited a rather weak inhibitory power and no significant differences were observed among them. Nor were any significant differences in the HPL surface density noted between any of the four

Table 1
Sandwich ELISA for measuring the biotinylated HGL* and HPL* interfacial binding[a]

Films	Lipases*	Lipase* concentration in recovered film (ng ml^{-1})	Lipase* concentration in bulk phase (ng ml^{-1})	Total recovery (%)	Lipase* activity (pmol cm^{-2} per min)	Lipase* surface concentration (pg cm^{-2})	Film adsorbed lipase* (%)	Specific activity of lipase* (μmol min^{-1} per mg)
1,2 Dicaprin	HGL*	116/114	91/86	92/87	133	395/442	0.40/0.44	318
	HPL*	7.1/6.3	3.9/3.1	57/46	21.7	42/40	0.62/0.59	529
A	HGL*	114/103	79/69	80/70	0	317/312	0.32/0.31	0.0
	HPL*	4.9/6.3	3.5/4.3	52/63	1.2	12/15	0.18/0.22	89
A′	HGL*	93/85	72/68	73/69	0	197/203	0.20/0.21	0.0
	HPL*	4.6/4.8	3.1/3.5	46/52	1.1	10/11	0.15/0.16	105
B	HGL*	107/97	65/58	66/59	3.1	353/328	0.36/0.33	9.0
	HPL*	4.2/4.9	3.4/3.5	50/52	2.6	17/14	0.25/0.21	168
B′	HGL*	90/95	70/79	71/80	0	230/184	0.23/0.18	0.0
	HPL*	4.7/4.4	2.9/3.1	43/46	2.2	22/12	0.32/0.18	129

[a] Biotinylated HGL* (6.8 ng ml^{-1}, final concentration) at pH 5 and biotinylated HPL* (99 ng ml^{-1}, final concentration) at pH 8, were recovered after 10 min incubation to monomolecular films (25 mN m^{-1}) of either 1,2-dicaprin or each pure enantiomeric inhibitor, A, A′, B, B′ depicted in Fig. 1. Each experiment was performed in duplicate. The surface of the reaction compartment was 100 cm^2 and its volume 100 ml (see chapter 2.6 and ref. [28] for calculation).

phosphonate inhibitors tested (Table 1). These results confirmed the low stereoselectivity of HPL using either triacylglycerols [29] or triacylglycerol analogues [27]. With HGL, however, the four organophosphorus enantiomers tested displayed differential inhibitory effects (Fig. 2(b)). The inhibition depended much more strongly on the chirality at the *sn*-2 carbon of the glycerol backbone, while the chirality at the phosphorus atom had no influence. Diastereomers A and B, which both contain the phosphorus moiety at the *sn*-3 position, were found to be the best inhibitors. This finding corroborates the *sn*-3 preference of HGL in the hydrolysis of acylglycerols [27–29]. Moreover, the HGL surface density levels varied significantly depending on the enantiomeric inhibitor used (Table 1). A clear correlation was observed between HGL surface concentration and the surface molar fraction (α_{50}) of inhibitor leading to half inhibition. The greatest enzymatic inhibition was observed with films containing the enantiomeric inhibitor to which HGL was best adsorbed (Table 2).

In order to describe the kinetics of lipolytic enzyme acting at an interface, a simple, adaptable model was proposed by Verger et al. [30] consisting of two successive equilibria (Fig. 3). The first

Table 2
Surface concentrations (Γ) of the biotin-labelled HGL* and HPL*, and inhibitor molar fraction leading to half inhibition (α_{50})[a]

Films	HGL* pH 5		HPL* pH 8	
	Γ (%)	α_{50}	Γ (%)	α_{50}
1,2-Dicaprin	100	–	100	–
A	80/71	0.05	29/37	0.20
A′	50/46	0.22	24/27	0.18
B	89/74	0.05	40/35	0.20
B′	58/42	0.22	52/30	0.13

[a] The surface concentrations of the biotinylated HGL* (2 nM, final concentration) at pH 5 and biotinylated HPL* (0.136 nM, final concentration) at pH 8 were expressed as the ratio, Γ%, of the amount of lipase adsorbed on each pure enantiomeric inhibitor, A, A′, B, B′, depicted in Fig. 1, to the amount of lipase adsorbed on 1,2-dicaprin films. The surface molar fraction (α_{50}) of each inhibitor, leading to half inhibition, was calculated from Fig. 2.

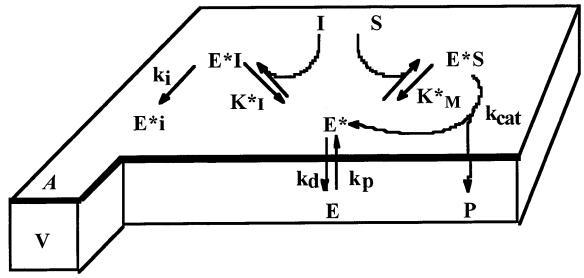

Fig. 3. Kinetic model illustrating the covalent inhibition of a lipolytic enzyme at a lipid/water interface. A, total interfacial area (surface); *V*, total volume (volume); E_0, total enzyme concentration (molecule/volume); *E*, free enzyme concentration (molecule/volume); *E**, interfacial enzyme concentration (molecule/surface); *S*, interfacial substrate concentration (molecule/surface); *I*, interfacial inhibitor concentration (molecule/surface); *P*, product concentration (molecule/volume); *E*S*, interfacial enzyme–substrate complex concentration (molecule/surface); *E*I*, interfacial enzyme–inhibitor complex concentration (molecule /surface); *E*i*, covalently inhibited enzyme concentration (molecule /surface); k_d, desorption rate constant (time^{-1}); k_p, penetration rate constant (volume surface^{-1} time^{-1}); k_{cat}, catalytic rate constant (time^{-1}); k_i, inhibition rate constant (time^{-1}); K^*_M, interfacial Michaelis–Menten constant (molecule/surface); K^*_I, interfacial dissociation constant for the enzyme–inhibitor complex (molecule/surface) [26].

describes the reversible penetration of a water soluble enzyme into an interface ($E \langle E^*$). This is followed by a second equilibrium, in which one molecule of penetrated enzyme binds to a single substrate molecule, forming the enzyme–substrate complex (E^*S). This is the two-dimensional equivalent of the classical Michaelis–Menten equilibrium. Once the complex (E^*S) has been formed, the catalytic steps take place, regenerating the enzyme in the (E^*) form and releasing the lipolytic products. An extension of the previous kinetic model was proposed by Ransac et al. for depicting the competitive inhibition [25], as well as the covalent inhibition [26] of lipolytic enzymes at a lipid/water interface.

With the phosphonate inhibitors tested during the present investigation, the experimentally recorded kinetic curves were found to be linear and not to show the sigmoidal pattern previously observed in the case of other lipase inhibitors [26]. This linearity could be explained by the above kinetic model, developed for covalent inhibition

of lipolytic enzymes, assuming a slow irreversible inhibition rate constant (k_i) as compared to the turn over rate constant (k_{cat}). In other words, we can use a *pseudo*-competitive kinetic model to interpret the data obtained with the weak ($\alpha_{50} \sim 0.2$) glycerophosphonate inhibitors. Since we are dealing with weak pseudo-competitive inhibitors, one can assume that K_M^* is small in comparison with K_I^*. Then, most of the interfacial lipase species present are in the (E^*) and (E^*S) forms, with negligible amounts in the (E^*I) form. Given this possibility, one could explain the important observation that the amount of adsorbed HGL depends on the chirality of the inhibitor enantiomer used (Table 2) by assuming the interfacial lipase binding is controlled by a supramolecular chiral recognition process, involving a lipid binding site which differs from the actual catalytic site. Alternatively, the chiral recognition may occur only at the active site, and these two hypotheses are non-mutually exclusive. In the latter case, all the interfacially bound lipase molecules will be complexed with the inhibitor in the (E^*S) form. This situation fits the classical chiral molecular recognition process, where all the enzyme molecules are stoichiometrically associated with a potent inhibitor. One has to realize, however, that up to now the experimentally determined interfacial excess of lipase molecules includes all the enzymatic species, (E^*), (E^*S) and (E^*I).

In the present study, the proportions of these enzymatic species were not determined and hence we are unable to strictly differentiate between the above two hypotheses. The present data do, however, seem to support the interfacial chiral recognition hypothesis in the case of a monomolecular homochiral film, but further experiments are required to substantiate this attractive theory, using for instance monofunctional chiral compounds with a negligible affinity to the lipase active site (chiral surface diluent).

Acknowledgements

This research was carried out under the BIOTECH G-Lipase (contract BIO2-CT94-3041) Program of the European Union.

References

[1] D. Andelman, J. Am. Chem. Soc. 111 (1989) 6536–6544.
[2] S. Pathirana, W.C. Neely, L.J. Myers, V. Vodyanoy, J. Am. Chem. Soc. 114 (1992) 1404–1405.
[3] E.M. Arnett, N.G. Harvey, P.L. Rose, Acc. Chem. Res. 22 (1989) 131–138.
[4] S. Patkar, F. Bjorkling, Lipase inhibitors, in: P. Wooley, S.B. Petersen (Eds.), Lipases. Their Structure, Biochemistry and Application, Cambridge University Press, Cambridge, UK, 1994, pp. 207–224.
[5] M.L.M. Mannesse, J.W.P. Boots, R. Dijkman, A.J. Slotboom, H.T.W.V. Vanderhijden, M.R. Egmond, H.M. Verheij, G.H. de Haas, Biochim. Biophys. Acta 1259 (1995) 56–64.
[6] P. Stadler, G. Zandonella, L. Haalck, F. Spener, A. Hermetter, F Paltauf, Biochim. Biophys. Acta 1304 (1996) 229–244.
[7] P. Grochulski, F. Bouthillier, R.J. Kazlauskas, A.N. Serreqi, J.D. Schrag, E. Ziomek, M. Cygler, Biochemistry 33 (1994) 3494–3500.
[8] P. Grochulski, Y. Li, J.D. Schrag, M. Cygler, Protein Sci. 3 (1994) 82–91.
[9] M. Cygler, P. Grochulski, R.J. Kazlauskas, J.D. Schrag, F. Bouthillier, B. Rubin, A.N. Serreqi, A.K. Gupta, J. Am. Chem. Soc. 116 (1994) 3180–3186.
[10] S. Longhi, M.L.M. Mannesse, H.M. Verheij, G.H. de Haas, M. Egmond, E. Knoops-Mouthuy, C. Cambillau, Protein Sci. 6 (1997) 275–286.
[11] F. Marguet, C. Cudrey, R. Verger, G. Buono, Biochim. Biophys. Acta 1210 (1994) 157–166.
[12] F. Marguet, Thesis. University of Aix-Marseilles III, Marseilles, France, 1994.
[13] M.-P. Egloff, F. Marguet, G. Buono, R. Verger, C. Cambillau, H. van Tilbeurgh, Biochemistry 34 (1995) 2751–2762.
[14] H. van Tilbeurgh, M.P. Egloff, C. Martinez, N. Rugani, R. Verger, C. Cambillau, Nature 362 (1993) 814–820.
[15] H. van Tilbeurgh, L. Sarda, R. Verger, C. Cambillau, Nature 359 (1992) 159–162.
[16] H. Moreau, C. Abergel, F. Carriere, F. Ferrato, J.C. Fontecilla-Camps, R. Verger, J. Mol. Biol. 225 (1992) 147–153.
[17] A. De Caro, C. Figarella, J. Amic, R. Michel, O. Guy, Biochim. Biophys. Acta 490 (1977) 411–419.
[18] M. Aoubala, C. Daniel, A. De Caro, M. G. Ivanova, M. Hirn, L. Sarda, R. Verger, Eur. J. Biochem. 211 (1993) 99–104.
[19] M. Aoubala, J. Bonicel, C. Benicourt, R. Verger, A De Caro, Biochim. Biophys. Acta 1213 (1994) 319–324.
[20] M.G. Ivanova, M. Aoubala, A. De Caro, C. Daniel, J. Hirn, R. Verger, Colloids Surf. B1 (1993) 17–22.
[21] R. Verger, G. H. de Haas, Chem. Phys. Lipids 10 (1973) 127–136.
[22] G. Pieroni, R. Verger, J. Biol. Chem. 254 (1979) 10090–10094.

[23] G. Pieroni, R. Verger, Eur. J. Biochem. 132 (1983) 639–644.
[24] Y. Gargouri, G. Pieroni, F. Ferrato, R. Verger, Eur. J. Biochem. 169 (1987) 125–129.
[25] S. Ransac, C. Riviere, J.M. Soulie, C. Gancet, R. Verger, G.H. de Haas, Biochim. Biophys. Acta 1043 (1990) 57–66.
[26] S. Ransac, Y. Gargouri, H. Moreau, R. Verger, Eur. J. Biochem. 202 (1991) 395–400.
[27] S. Ransac, E. Rogalska, Y. Gargouri, A.M.T.J. Deveer, F. Paltauf, G.H. de Haas, R. Verger, J. Biol. Chem. 265 (1990) 20263–20270.
[28] M. Aoubala, M. G. Ivanova, I. Douchet, A. de Caro, R. Verger, Biochemistry 34 (1995) 10786–10793.
[29] E. Rogalska, C. Cudrey, F. Ferrato, R. Verger, Chirality 5 (1993) 24–30.
[30] R. Verger, M.C.E. Mieras, G.H. de Haas, J. Biol. Chem. 248 (1973) 4023–4034.